Title:
Model-based Next-best-view Planning of Terrestrial Laser Scanner for HVAC Facility Renovation

Authors:
Eisuke Wakisaka, wakisaka.ei@shinryo.com, Shinryo Corporation
Satoshi Kanai, kanai@ssi.ist.hokudai.ac.jp, Hokkaido University
Hiroaki Date, hdate@ssi.ist.hokudai.ac.jp, Hokkaido University

Keywords:
Next-best-view Planning, Laser Scanning, Structure-from-Motion, Terrestrial Laser Scanner, As-built Modeling

DOI: 10.14733/cadconfP.2017.227-231

Introduction:
Recently, building facility renovations have been increasing in the heating, ventilating, and air conditioning (HVAC) industries. Additionally, the reconstruction of as-built 3D models of facilities by laser scanning using a terrestrial laser scanner (TLS) has enabled shorter survey periods and in-depth construction planning. More accurate and efficient on-site laser scanning is currently required for the as-built 3D modeling of HVAC facilities. However, the accuracy of scanned points primarily depends on the incident angle of the laser beam on the object surfaces and the scan range [5]. For registration, the scanned points must have a certain amount of overlap among them. Furthermore, because the system scanning priority considerably differs according to local region and type of construction work, a typical scanner placement that makes it possible to scan all objects in the site without omission is impractical. Hence, in laser scanning for HVAC facilities, an optimum scanner placement is required that satisfies all aspects of scan quality, such as incident angle, scan range, and scan overlap, given the scanning priority and also minimizes the number of scans and amount of occlusion. However, scanner placement is currently decided manually by operators. In addition, there is no guarantee that their placement minimizes the number of scans and completely fulfills the required scan quality.

Planning optimal sensor placements is known as the next-best-view (NBV) problem, and an NBV planning for TLS was studied for modeling piping facilities [3]. However, the plan in this study ignores the constraints on scan quality and does not actualize the most efficient scanner placement because of the lack of a-priori knowledge. An NBV planning for TLS was proposed for modeling outdoor buildings with a structure-from-motion (SfM) model as a-priori knowledge [4]. However, the scan quality is not directly considered. An NBV planning for heritage sites was also proposed wherein a 2D map was used for a-priori knowledge and scan quality was considered [1]. However, the plan could not actualize full scan coverage because of 3D self-occlusions when overlapping HVAC facilities are scanned.

To solve these problems, we propose a new TLS NBV planning method for the as-built modeling of HVAC facilities. In this method, an SfM model is used as a rough 3D a-priori knowledge of the as-built HVAC facilities and a near-optimal TLS placement wherein the number of scans is minimized while considering both scan quality and scan priority can be derived. Comparing the scanner placement obtained by our method with that obtained by an operator, the effectiveness of the proposed method is experimentally validated.

NBV planning method:
Overview of the Proposed Method

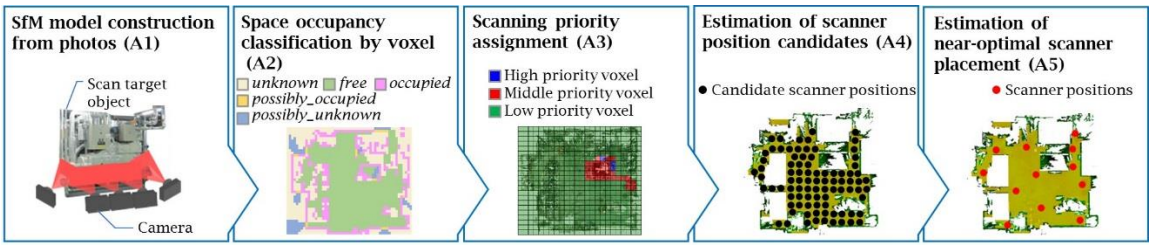

Fig. 1: Overview of the proposed method.

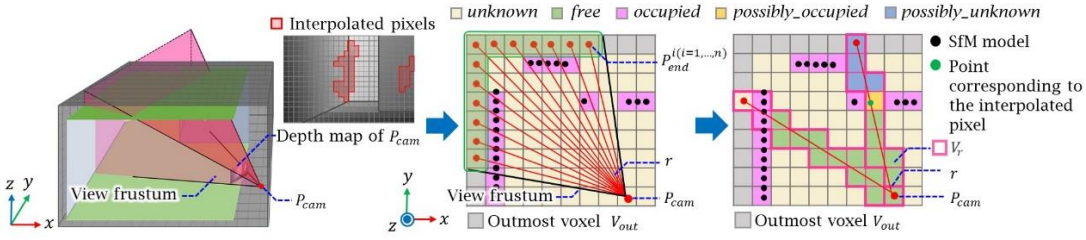

Fig. 2: Spatial occupancy classification using depth maps.

Fig. 1 shows an overview of the proposed method. First, a rough model (SfM model) of the space to be scanned is constructed from multiple photos during a preliminary survey (A1). Next, the space including the model is decomposed into a set of voxels and space occupancy is classified by ray-casting at the camera positions estimated by the SfM (A2). Scanning priorities that differ by region depending on the type of the construction are assigned to voxels interactively (A3). Then, practical scanner position candidates are estimated based on the space occupancy (A4). Finally, a near-optimal scanner placement is extracted from the position candidates that minimizes the number of scans, maximizes coverage, and satisfies the constraints of incident angle, scan range, and scan overlap (A5).

SfM Model Construction from Photos (A1)

To obtain a-priori knowledge of the space to be scanned, an SfM model is generated from multiple photos using commercial SfM software. However, when applying SfM to indoor HVAC facilities, the model usually includes multiple defects, such as holes, because of the lack of feature points in the photos. Because false classifications occur when spatial occupancy is classified using this model and a poor scanner position might be obtained, these defects are rectified by our algorithm described in A2.

Spatial Occupancy Classification by Voxel (A2)

When planning the scanner placement, the free or occupied status of the space to be scanned needs to be determined. Hence, the space enclosing the SfM model is decomposed into a set of voxels and a spatial occupancy attribute is assigned to each voxel. First, to rectify the defects in the SfM model, a depth map is generated at a camera position estimated by the SfM software. Next, depth values at the defects are interpolated using the neighboring depth values based on color similarity among image pixels. We adopted the depth map-restoring approach of Bapat et al. [2].

Then, as shown in Fig. 2, the interpolated depth in the map at each camera position is back-projected to the voxel space and ray-casting is performed between the projection centers of the camera P_{cam} and the outmost voxel centroid P_{end} contained in the view frustum. Consequently, the spatial occupancy attribute $a(v) \in \{free, occupied, unknown, possibly\_occupied, possibly\_unknown\}$ is assigned to a voxel v. As shown in Fig. 2, $a(v) = free$ indicates that a ray from the camera has already passed through the voxel v and that v contains no object. Further, $a(v) = occupied$ indicates that v contains a surface of the SfM model, $a(v) = possibly\_occupied$ indicates that v contains a point corresponding to an interpolated depth, and $a(v) = unknown$ and $a(v) = possibly\_unknown$ indicate that a ray from the camera has not yet passed through v because it is blocked by an *occupied* and *possibly_occupied* voxel, respectively. Initially, $a(v) = unknown$ is assigned to all voxels. By collecting all of *occupied* voxels $a(v) = occupied$, a set of scan target voxels V_o is finally determined.

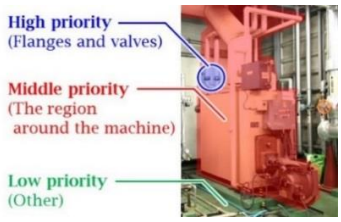

Fig. 3: Scanning priority levels.

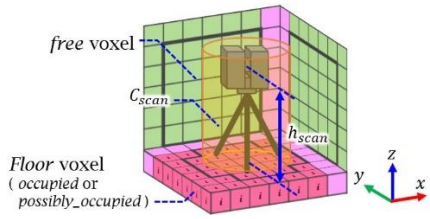

Fig. 4: Candidate scanner positions.

Scanning Priority Assignment (A3)

In facility construction, scanning priority differs by region depending on the type of the construction. For example, as shown in Fig. 3, in case of a laser scan for updating equipment, the flanges and valves connecting the equipment and pipes should be assigned $high$ priority because their scanned points must have precise positional information and satisfy the conditions of scan quality. In contrast, the regions around the equipment should be assigned $middle$ priority because the interference between the new pipes and the equipment only has to be inspected in the scan without considering scan quality constraints. The other regions are assigned low priority, and no measurements are needed. In the priority assignment, first, the SfM model is interactively segmented into several regions using point cloud-processing software. Then, the scanning priority $b(v) \in \{high, middle, low\}$ is interactively assigned to each occupied voxel v_{occ} included in each segment.

Estimation of Scanner Position Candidates (A4)

Here, a set of candidates for scanner positions is extracted from the voxel space wherein a scanner can practically be placed. First, the average normal of the faces on the SfM model in a voxel $\boldsymbol{n}_z$ is estimated. Next, a voxel whose normal vector $\boldsymbol{n}_z$ points vertically upward is extracted as a $floor$ voxel from $occupied$ voxels $a(v) = occupied$. Subsequently, the connected $floor$ voxels are clustered using Euclidian clustering.

To find the scanner position candidates, as shown in Fig. 4, the shape of a laser scanner body including a tripod is approximated by an enclosed cylinder C_{scan}. Then, only the subset of $floor$ voxels on which the scanner can be placed are extracted according to the following two conditions. The first is that the voxels at the bottom of C_{scan} are $occupied$ voxels ($a(v) = occupied$) or $free\_occupied$ voxels ($a(v) = free\_occupied$). The second is that C_{scan} should not include any $occupied$ voxel within it, except for $floor$ voxels, to avoid a collision between the scanner body and other objects. Then, a $free$ voxel that is located above the $floor$ voxel and whose height equals the scanner origin height h_{scan} is selected as the scanner position candidate voxel v_c. By collecting all values of v_c at every position of C_{scan} in the voxel space, a set of scanner position candidate voxels V_c is finally determined.

Estimation of Near-optimal Scanner Placement (A5)

Finally, a sequence of near-optimal scanner placements is searched, each placement of which maximizes the coverage of the voxels in V_o while satisfying the following constraints on the incident angle, scan range, scan overlap, and visibility condition. For this optimization, the greedy method is adopted.

1) The incident angle constraint can be expressed as follows:

$$ang\{r(v_c, v_o), \boldsymbol{n_z}(v_o)\} \leq \theta_\alpha \tag{1}$$

where $r(v_c, v_o)$ denotes a line segment connecting v_c and v_o and θ_α is the maximum allowable incident angle.

2) The scan range constraint can be expressed as follows:

$$d_{min} < dist(v_c, v_o) \leq d_{max} \tag{2}$$

where $dist(v_c, v_o)$ denotes the distance between v_c and v_o and d_{min} and d_{max} represent the minimum and maximum allowable distance of scan range, respectively.

3) The scan overlap constraint can be expressed as follows:

$$\frac{\left|V_{occ}^{i-1}(v_c) \cap V_m^i(v_c)\right|}{\left|V_m^i(v_c)\right|} \geq \tau_o \tag{3}$$

where $V_{occ}^{i-1}(v_c)$ denotes a subset of occupied voxels captured until $i-1$th scan, $V_m^i(v_c)$ is a subset of occupied voxels captured at the i-th scan, and τ_o is the minimum scan overlap rate.
4) The visibility condition can be expressed as follows:

$$\prod_{v_l \in V_l} p(v_l) > 0 \tag{4}$$

where $p(v_l)$ is a probability representing the extent to which a laser beam of the scanner l can penetrate the voxel v_l in the set of voxels V_l that are intersected by a laser beam l between v_c and v_o. The probability $p(v_l)$ is also given as 1.0 for $a(v_l) = free$, 0.0 for $a(v_l) = occupied$, 0.5 for $a(v_l) = unknown$, 0.5 for $a(v_l) = possibly\_occupied$, and 0.75 for $a(v_l) = possibly\_unknown$.

A scan completion attribute $c(v) \in \{measured, unmeasured\}$ is additionally assigned to each scan target voxel v_o. Initially, $unmeasured$ is assigned to all scan target voxels. In the search for the scanner placement, first, a voxel with $b(v_o) = high$ is selected as a scan target voxel to create a scan target voxel set V_o. Next, ray-casting is performed between v_c and v_o and the number of scan target voxels $N(v_c)$ is counted if the voxel satisfies the scan quality of Eqns. (1)–(3) and the visibility condition of Eqn. (4). This $N(v_c)$ is evaluated at every scanner position candidate voxel v_c, and the value of v_c that maximizes $N(v_c)$ is determined to be the optimal scanner position v_{opt}^i at the i-th scan. Finally, ray-casting is performed between v_{opt}^i and v_o and the scan completion attribute $c(v_o)$ of the target voxel v_o satisfying Eqn. (1), (2), and (3) is updated to $measured$. This process is repeated until the change in the number of the scan target voxels with $c(v_0) = measured$ converges. Subsequently, a similar process is executed again for the other scan target voxels v_o with $b(v_o) = middle$. As a result, a sequence of near-optimal scanner placements is determined such that the ratio of the total number of scan target voxels with $c(v_0) = measured$ to that of all voxels in V_o (the scan coverage) is maximized.

Results and Conclusion:

Fig. 5 and Fig.6 shows an SfM model of a heat source machine room and its scanning priorities respectively. The scanning condition of the commercial TLS (Imager5010c, Z+F) shown in Tab.1 was used in the proposed NBV method. Different-typed scanner can be simulated by changing these setting.

Scanning condition	*Value*
Scanner height h_{scan}	1.4 [m]
Scanner radius r_{scan}	0.3 [m]
Vertical field of view	320 [deg]
Horizontal field of view	360 [deg]
Vertical scan pitch	0.072[deg]
Horizontal scan pitch	0.072[deg]

Tab.1: Scanning condition used.

To examine the effectiveness of the method, a near-optimal scanner placement was obtained using the proposed NBV method, unconstrained NBV method, and by an experienced operator having four years of experience in scanning projects. The proposed NBV method completely complied with the all constraints. For the scan quality constraints, we specified $\theta_\alpha = 45°$, $d_{min} = 0.3$ m, $d_{max} = 5.0$ m, and $\tau_o = 20\%$. By contrast, the unconstrained NBV method complied with the original visibility constraint of Eqn. (4) and the other constraints with loose settings. Then, to compare as-built modeling accuracy, we conducted the scanning operations from the setup positions obtained both by proposed method and the unconstrained one. Using Levenberg-Marquardt method, cylinders with end faces were finely fitted to point clouds on ten flanges to which high priority level was assigned, and their center positions were estimated. These center positions were measured separately by a high-accuracy Total Station and were used as reference positions to evaluate the positional errors of the as-built models of the flanges.

Fig. 7 indicates the scanner placements obtained by the three methods. Fig. 8 shows the change in the coverage of the voxels meeting the constraints for each scan. The coverage obtained by the proposed NBV method was better than that obtained by the unconstrained NBV method and the operator for every scan. In particular, when the scan quality constraints are considered, the scanner placement of the proposed method achieved 88.0% coverage, whereas that of the operator only covered 59.6% of the scan target voxels. Additionally, the estimation of the scanner placement in both cases described in Fig. 6(a) and (b) required around 50 min using a standard PC, except for the manual processes of A1 and A3. Finally, the positional errors at the end-face's centers of as-built flange models were compared among the three methods. As shown in Fig. 9, the proposed NBV method exhibits the smallest maximum and average errors among three methods, and most of positional errors in the proposed method fall within the practical allowance (5mm) of HVAC renovation works.

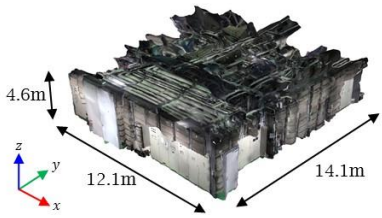

Fig. 5: SfM model of heat source machine room.

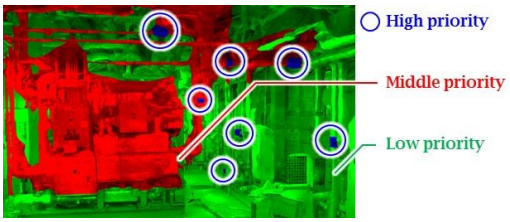

Fig. 6: Priority levels assigned to SfM model.

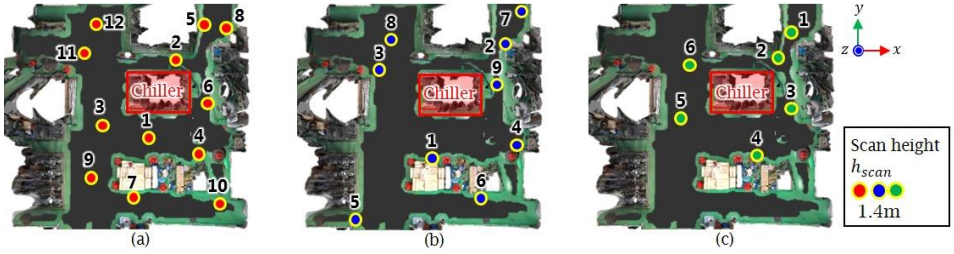

Fig. 7: Scanner placement obtained by (a) the proposed NVB method, (b) the unconstrained NBV method, and (c) an experienced operator.

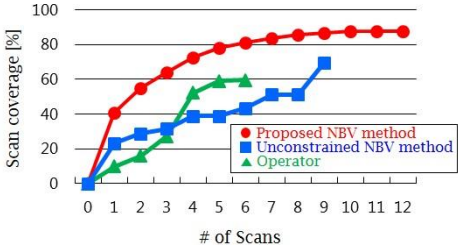

Fig. 8: Change in scan coverage of voxels meeting the constraints for each scan.

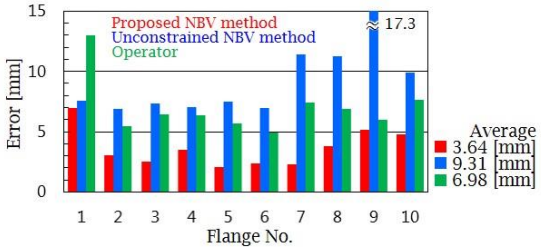

Fig. 9: Measurement error of the center position of end face of flanges.

These results demonstrate that the proposed NBV planning method is effective for finding an optimum TLS placement which realizes larger amount of scan coverage and better as-built modeling accuracy of HAVC facilities than the scanner placement determined by experienced operators.

References:

[1] Ahn, J.; Wohn, K.: Interactive scan planning for heritage recording, Multimedia Tools and Applications, 2016, 1-21. http://dx.doi.org/10.1007/s11042-015-2473-0

[2] Bapat, A.; Ravi, A.; Raman, S.: An iterative, non-local approach for restoring depth maps in RGB-D images, Communications (NCC), 2015 Twenty First National Conference on. IEEE, 2015, 1-6. http://dx.doi.org/10.1109/NCC.2015.7084819

[3] Kawashima, K.; Yamanishi, S.; Kanai, S.; Date, H.: Finding the next-best scanner position for as-built modeling of piping systems, The International Archives of the Photogrammetry Remote Sensing and Spatial Information Sciences, KL-5, 2014, 313-320. http://dx.doi.org/10.5194/isprsarchives-XL-5-313-2014

[4] Kitada, Y.; Dan, H., Yasumuro, Y.: Optimization scenario for 3D-scanning plans of outdoor constructions based on SFM, Proc. of the 15th International Conference on Construction Applications of Virtual Reality, 2015, 65-68.

[5] Soudarissanane, S.; Lindenbergh, R.; Menenti, M.; Teunissen, P.: Incidence angle influence on the quality of Terrestrial Laser Scanning points, Proceedings of ISPRS Workshop Laser Scanning 2009, 2009, 183-188.